

Microelectromagnets for Trapping and Manipulating Ultracold Atomic Quantum Gases

J. Fortágh, H. Ott, G. Schlotterbeck, and C. Zimmermann
*Physikalisches Institut der Universität Tübingen
 Auf der Morgenstelle 14, Tübingen, Germany*

B. Herzog, and D. Wharam
*Institut für Angewandte Physik, Universität Tübingen
 Auf der Morgenstelle 10, Tübingen, Germany*
 (November 12, 2018)

We describe the production and characterization of microelectromagnets made for trapping and manipulating atomic ensembles. The devices consist of 7 fabricated parallel copper conductors $3\text{ }\mu\text{m}$ thick, 25 mm long, with widths ranging from $3\text{ }\mu\text{m}$ to $30\text{ }\mu\text{m}$, and are produced by electroplating a sapphire substrate. Maximum current densities in the wires up to $6.5 \times 10^6\text{ A cm}^{-2}$ are achieved in continuous mode operation. The device operates successfully at a base pressure of 10^{-11} mbar . The microstructures permit the realization of a variety of magnetic field configurations, and hence provide enormous flexibility for controlling the motion and the shape of Bose-Einstein condensates.

The combination of ultracold atoms and miniaturized magnetic traps [1] suggests fascinating scenarios for integrated atom optic devices including waveguides, interferometers, resonators, and quantum gates [2]. The current progress in reducing the production time of Bose-Einstein condensates below 1 s [3] and the recently achieved significant simplification of the magnetic apparatus [4] adds to the vision of a future quantum technology with coherent matter waves analogous to today's highly developed laser technology. One of the crucial prerequisites is the preparation of atomic clouds in steep potentials. As a particularly attractive approach, magnetic fields generated by miniaturized current conductors can be used [5]. In addition, the trapping potentials can be spatially structured on a micron length scale and temporal modulations are possible on the scale of microseconds. By using miniaturized conductors, the trapping potential is located close to the surface of the substrate. At a distance of about $100\text{ }\mu\text{m}$ from the surface loss mechanisms, heating and decoherence effects within the cloud are predicted to become significant [6]. Earlier experiments succeeded in loading atoms into microtrap potentials that were generated by current conductors on the scale of several $10\text{ }\mu\text{m}$ [7]. Microtraps based on smaller conductors have been demonstrated electrically [8], and single atoms have been successfully guided in a micro magnetic channel [9]. In this Letter we describe the realization of magnetic microtraps with ultra thin conductors that reach the limit of surface-atom-interaction. Details of the fabrication pro-

cedure, and the chemical and electrical properties are given. The particular microstructure described has been used for generating highly anisotropic Bose-Einstein condensates [4]. We give a brief summary of the experiments and conclude with an estimation of the field configurations which can be reached with this device.

The microelectromagnet consists of a parallel configuration of copper wires with widths ranging from $3\text{ }\mu\text{m}$ to $30\text{ }\mu\text{m}$. The thickness of the galvanically deposited copper was of the order of a few microns, while the length of the total structure was approximately 25 mm.

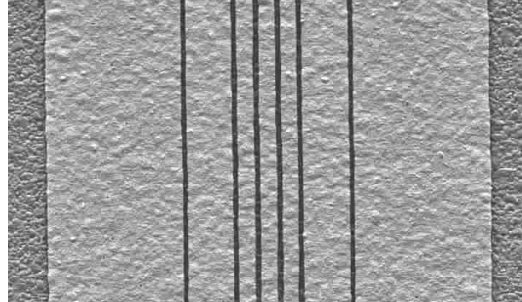


FIG. 1. An electron micrograph of a typical microtrap showing a segment of the wire geometry employed. The wire widths are $30\text{ }\mu\text{m}$, $11\text{ }\mu\text{m}$, and $3\text{ }\mu\text{m}$, and the nominal separation between wires is $1\text{ }\mu\text{m}$. The quality of the electroplating can be seen in the smoothness of the copper wires. The residual roughness is presumably due to the roughness of the sapphire substrate.

The fabrication of thin metallic wires with such high aspect ratios and excellent conducting properties requires the use of sophisticated microfabrication techniques. Initially, a high-quality optical mask was prepared using electron-beam lithography, which was then employed to transfer the wire pattern onto the smooth (residual roughness $\leq 1\text{ }\mu\text{m}$) sapphire substrate. In order to guarantee good adhesion and to provide a contact layer for the subsequent galvanic processing the substrate was also coated with a thin (7 nm Cr followed by 120 nm Cu) metallic layer by thermal evaporation. The wire fabrication itself was performed in a conventional acidic CuSO_4 galvanic bath with an additional organic brightener which produces copper layers of high-

purity ($\geq 99.99\%$) and a density of 8.9 g cm^{-3} . Best results were obtained using the technique of pulsed plating where the current was modulated with a square wave of frequency 1 kHz and current values of 360 mA and -40 mA for the positive and negative excursions respectively. This technique is well suited for the fabrication of smooth metallic layers as evidenced by the finished structure shown in Fig. 1.

For the chosen cathode area (ca. 44 cm^2) the above conditions correspond to a current density of approximately 0.8 A dm^{-2} (and -0.09 A dm^{-2} for the negative half-cycle), and to an electroplating rate of 1 nm s^{-1} . After removal of the photoresist the metallic contact layer was chemically etched with nitric acid for copper removal followed by potassium ferricyanide for the chrome removal. The quality of the electroplated layer and substrate was confirmed via EDX measurements which show neither the presence of magnetic impurities nor significant contamination.

A test structure with a $1.6 \mu\text{m}$ copper layer was used to determine the critical current at which the conductors are thermally damaged. The measurements were carried out at room temperature in air with the microstructure mounted on a copper heat sink. The electrical contact to the microstructure is accomplished by bonding 3 aluminium wires with $20 \mu\text{m}$ diameter and a length of about $700 \mu\text{m}$ onto each contact. Roughly 10 s after changing the current in the conductors a steady state temperature is reached, and the voltage drop along the wires can be recorded. Thus the current was increased every 10 s in steps of 10 mA for the $3 \mu\text{m}$ -conductor and in steps of 50 mA for $11 \mu\text{m}$ - and $30 \mu\text{m}$ -conductors. The maximum stable current is marked by the last data point in Fig. 2, which shows the device resistance as a function of the current.

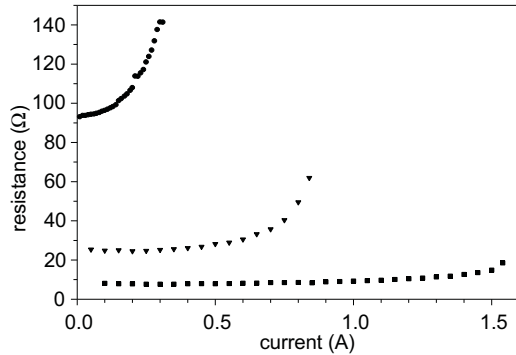


FIG. 2. The device resistance is plotted as a function of the driving current for three different wire widths $3 \mu\text{m}$ (○), $11 \mu\text{m}$ (▽), and $30 \mu\text{m}$ (□). The characteristics stop at the last measurable point before thermal damage leads to device breakdown.

The corresponding maximum current densities are $3.1 \times 10^6 \text{ A cm}^{-2}$, $4.8 \times 10^6 \text{ A cm}^{-2}$, and $6.5 \times 10^6 \text{ A cm}^{-2}$ for the $30 \mu\text{m}$, $11 \mu\text{m}$, and $3 \mu\text{m}$ conductors respectively.

The maximum current density increases with decreasing width, presumably because the geometry of thinner conductors favours a more efficient heat contact with the substrate. The resistance increases by a factor of 2.5 and of 2.3 respectively which corresponds to a temperature increase of about 350 K, determined using the thermal coefficient of resistance for bulk copper ($\alpha = 0.004 \text{ K}^{-1}$). We therefore estimate that the average temperature of the wires at breakdown is roughly 650 K. Near imperfections, which may be caused by unintentional variations of the conductor cross section or by reduced adhesion to the substrate, we expect the temperature to exceed the average value and to lead to breakdown when the local temperature reaches the melting point of bulk copper (1350 K). The temperature behaviour near the maximum current is similar for the $11 \mu\text{m}$ and $30 \mu\text{m}$ conductors. The resistance of the $3 \mu\text{m}$ conductor increases only by a factor of 1.5 at the maximum current and the average temperature is increased to only 450 K. This can be explained by a stronger influence of the imperfections. The maximum current densities measured in our test experiments at room temperature are similar to the critical current densities in high- T_c superconductors at liquid nitrogen temperature [5] and fall short only by a factor 15 of the values obtained by Drndic et al. [8] with gold conductors on sapphire substrates at liquid helium temperature. The microelectromagnets are used under ultra-high vacuum conditions and can be cooled with liquid nitrogen. A significant resistance reduction and consequent increase in critical current density is observed. In addition, the cooling reduces outgassing of the surface and results in longer lifetimes of the trapped atoms. Nevertheless the longest lifetimes observed in recent experiments [12] depend critically upon the separation between substrate and condensate; for separations of $200 \mu\text{m}$ and $20 \mu\text{m}$ lifetimes of 15 s and 700 ms respectively were found.

The configuration of seven parallel conductors with different widths combined with the extreme length of the microstructure of 25 mm permits the definition of a variety of magnetic trapping potentials [4]. Besides the usual magnetic traps used for Bose-Einstein condensation, very elongated waveguides can also be obtained by changing the current in the microstructure. Furthermore, a parallel set of waveguides can be formed and may be merged and separated by varying the strength of the offset field perpendicular to the waveguides [13]. Such configurations permit the realization of on-chip interferometers, and are currently the subject of investigation.

In order to achieve the Bose-Einstein condensation [4] one conductor is driven for example with an current source of 0.2 A, and an external bias field of 4 G is applied. The resulting gradient in this instance amounts to 400 G cm^{-1} and the center of the trap is located $100 \mu\text{m}$ above the surface of the microstructure. With a superimposed offset field of 1 G aligned parallel to the conductor the curvature of the magnetic field magnitude in the transverse direction amounts to 16 kG cm^{-2} corresponding to a radial (transverse) oscillation frequency of

$\omega_r = 2\pi \times 510 \text{ s}^{-1}$ for ^{87}Rb atoms in the $|F=2, m_F=2\rangle$ ground state. The axial (longitudinal) confinement of the atoms is separately controlled by an additional Ioffe-type electromagnet [10], which is adjusted such that the axial oscillation frequency amounts to $\omega_a = 2\pi \times 14 \text{ s}^{-1}$. The atoms are loaded into the microtrap by adiabatic compression [1] and subsequently cooled below the critical temperature by forced rf-evaporation. Condensation is reached with 10^6 atoms at a temperature of $1 \mu\text{K}$. This standard trap configuration can be continuously changed into a much steeper potential with an elongated waveguide of large aspect ratio. In the particular experiment shown in Fig. 3 the axial oscillation frequency of the trap was reduced by a factor of 10 on a timescale of 400 ms. During the last 100 ms the trap center was shifted by 1 mm such that the condensate is free to propagate along the waveguide. This motion is clearly visible, and observations over longer time scales show oscillations of the center of mass of the condensate at the trap frequency of $2\pi \times 1.4 \text{ s}^{-1}$. The distance to the surface and the radial oscillation frequency were tuned to $270 \mu\text{m}$ and $2\pi \times 100 \text{ s}^{-1}$ accordingly.

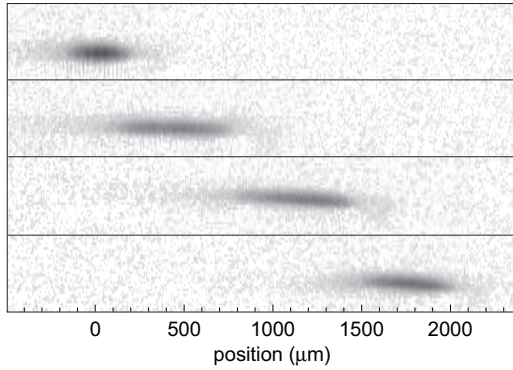


FIG. 3. The time evolution of the Bose-Einstein condensate is shown at $t = 0 \text{ ms}$, $t = 100 \text{ ms}$, $t = 200 \text{ ms}$, and $t = 300 \text{ ms}$ respectively. The trap was turned off 20 ms before the first image of the condensate was obtained and after the potential modification described in the text was complete. The number of atoms in the condensate is estimated to be 1.5×10^5 .

In the most extreme potential configuration obtainable with our microstructure, defined by the maximum current density and the size of the thinnest conductor, the magnetic field gradient is expected to reach 500 kG cm^{-1} . With a current of 200 mA in the center conductor and -325 mA in both of the two neighboring conductors the trap is located $3 \mu\text{m}$ above the surface and has a depth of 133 G corresponding to a temperature of 8 mK for ^{87}Rb atoms. With an axial offset field of 1 G, the radial curvature amounts $2.5 \times 10^{11} \text{ G cm}^{-2}$ corresponding to an oscillation frequency of $\omega_r = 2\pi \times 600,000 \text{ s}^{-1}$. By choosing a small axial oscillation frequency (for example $\omega_a < 2\pi \times 5 \text{ s}^{-1}$), an aspect ratio of $\omega_r/\omega_a > 100,000$ can be achieved. To date, the properties of cold atomic ensembles have not been investigated under such extreme

conditions due to the lack of an appropriate device. In our most recent experiments we observe periodic substructures in the spatial distribution of an elongated condensate at a surface separation below $150 \mu\text{m}$, which is reported in detail elsewhere [12,14]. The obvious causes for such modulated magnetic or electrostatic potentials have been excluded, and we speculate that their origin lies in the magnetic surface properties of the conductors.

In conclusion, we have demonstrated a device for the manipulation of Bose-Einstein condensates based on microfabricated electromagnets. The microfabrication technique employed allows the construction of even more sophisticated micromagnets, and opens new possibilities for integrated atom-optical devices with ultracold atoms. Novel sensors for rotation and for precision measurement of the gravitational field may become feasible.

ACKNOWLEDGMENTS

This work is supported in part by the Deutsche Forschungsgemeinschaft under grant no. Zi 419/3-1. We thank S. Raible and R. Frank for technical assistance, and HighFinesse for providing ultra stable current sources for driving the microelectromagnet.

- [1] V. Vuletic, T. Fischer, M. Praeger, T. W. Hänsch, and C. Zimmermann, Phys. Rev. Lett. **80**, 1634 (1998), J. Fortágh, A. Grossmann, T.W. Hänsch, and C. Zimmermann, Phys. Rev. Lett. **81**, 5310 (1998).
- [2] R. Folman, P. Krüger, D. Cassettari, B. Hessmo, T. Maier, and J. Schmiedmayer, Phys. Rev. Lett. **84**, 4749 (2000), W. Hänsel, J. Reichel, P. Hommelhoff, and T.W. Hänsch, Phys. Rev. Lett. **86**, 608 (2001).
- [3] W. Hänsel, P. Hommelhoff, T.W. Hänsch, and J. Reichel, Nature **412**, 498 (2001), M.D. Barrett, J.A. Sauer, and M.S. Chapman, Phys. Rev. Lett. **87**, 010404 (2001).
- [4] H. Ott, J. Fortágh, G. Schlotterbeck, A. Grossmann, and C. Zimmermann, Phys. Rev. Lett. **87**, 230401 (2001).
- [5] J.D. Weinstein and K.G. Libbrecht, Phys. Rev. **A52**, 4004 (1995).
- [6] C. Henkel and M. Wilkens, Europhys. Lett. **47**, 414 (1999).
- [7] J. Fortágh, A. Grossmann, T.W. Hänsch, and C. Zimmermann, Phys. Rev. Lett. **81**, 5310 (1998), J. Reichel, W. Hänsel, and T.W. Hänsch, Phys. Rev. Lett. **83** 3398 (1999), D. Müller, D.Z. Anderson, R.J. Grow, P.D.D. Schwindt, and E.A. Cornell, Phys. Rev. Lett. **83**, 5194 (1999), M. Key, I.G. Hughes, W. Rooijakkers, B.E. Sauer, E.A. Hinds, D.J. Richardson, and P.G. Kazansky, Phys. Rev. Lett. **84**, 1371 (2000), N.H. Dekker, C.S. Lee, V. Lorent, J.H. Thywissen, S.P. Smith, M. Drndic, R.M. Westervelt, and M. Prentiss, Phys. Rev. Lett. **84**, 11124

(2000), D. Cassettari, B. Hessmo, R. Folman, T. Maier, and J. Schmiedmayer, Phys. Rev. Lett. **85**, 5483 (2000).

[8] M. Drndic, K.S. Johnson, J.H. Thywissen, M. Prentiss, and R.M. Westervelt, Appl. Phys. Lett. **72**, 2906 (1998).

[9] J.H. Thywissen, M. Olshanii, G. Zabow, M. Drndic, K.S. Johnson, R.M. Westervelt, and M. Prentiss, Eur. Phys. J. **D7**, 361 (1999).

[10] J. Fortágh, H. Ott, A. Grossmann, and C. Zimmermann, Appl. Phys. **B70**, 701 (2000).

[11] W. Hänsel, J. Reichel, P. Hommelhoff, and T.W. Hänsch, Appl. Phys. **B72**, 81 (2001).

[12] J. Fortágh, H. Ott, S. Kraft, and C. Zimmermann, cond-mat/0205310

[13] E.A. Hinds, C.J. Vale, and M.G. Boshier, Phys. Rev. Lett. **86**, 1462 (2001).

[14] A.E. Leanhardt, A.P. Chikkatur, D. Kielpinski, Y. Shin, T.L. Gustavson, W. Ketterle, D.E. Pritchard, cond-mat/0203214